Original Research Paper

Intra-Articular injection of acid-sensitive stearoxyl-ketal-dexamethasone microcrystals for long-acting arthritis therapy

Yang Xu [a,1], Ziqi Chen [a,1], Zunkai Xu [a], Yanyan Du [b], Jianghao Han [a], Xiaoyong Yuan [c,*], Shubiao Zhang [b,*], Shutao Guo [a,*]

[a] Key Laboratory of Functional Polymer Materials of Ministry of Education, State Key Laboratory of Medicinal Chemical Biology and Institute of Polymer Chemistry, College of Chemistry, Nankai University, Tianjin 300071, China
[b] Key Laboratory of Biotechnology and Bioresources Utilization of Ministry of Education, Dalian Minzu University, Dalian 116600, China
[c] Clinical College of Ophthalmology, Tianjin Medical University, Tianjin Eye Hospital, Tianjin Key Laboratory of Ophthalmology and Visual Science, Tianjin Eye Institute, Tianjin 300022, China

ARTICLE INFO

ABSTRACT

Despite advances in treatment of chronic arthritis, there is still a strong need for the development of long-acting formulations that can enable local and sustained drug release at the inflamed tissues. In this work, we fabricated microcrystals of an acid-sensitive stearoxyl-ketal-dexamethasone prodrug for treatment of arthritis. Microcrystals of the prodrug with two sizes were successfully engineered and showed pH-dependent hydrolysis kinetics *in vitro*. In a collagen-induced arthritis rat model, we evaluated the influence of particle size and injection dose on anti-inflammatory effect after intra-articular injection. Such prodrug demonstrated long-acting anti-arthritis effects with good safety. Our results indicate ketal-based prodrugs are promising for the development of long-acting injectables and may stimulate the development of new treatments for chronic diseases.

1. Introduction

Chronic arthritis, such as rheumatoid arthritis (RA) and osteoarthritis (OA), is a type of widespread and incurable diseases and affects more than 4% global population [1,2]. They are characterized by sustained synovitis, progressive cartilage and bone destruction, and often cause severe pain and disability [3,4]. Glucocorticoids are classic drugs for clinical relief of arthritis symptoms [5,6]. However, long-term daily oral or intravenous glucocorticoid treatments lead to patient noncompliance and severe systemic side effects, such as hyperglycemia, hypertension and Cushing syndrome [7,8]. To reduce side effects and improve therapeutic efficacy, local sustained-release formulations would be highly desirable.

---

* Corresponding authors.
   E-mail addresses: yuanxy_cn@hotmail.com (X.Y. Yuan), zsb@dlnu.edu.cn (S.B. Zhang), stguo@nankai.edu.cn (S.T. Guo).
[1] These authors contributed equally to this work.
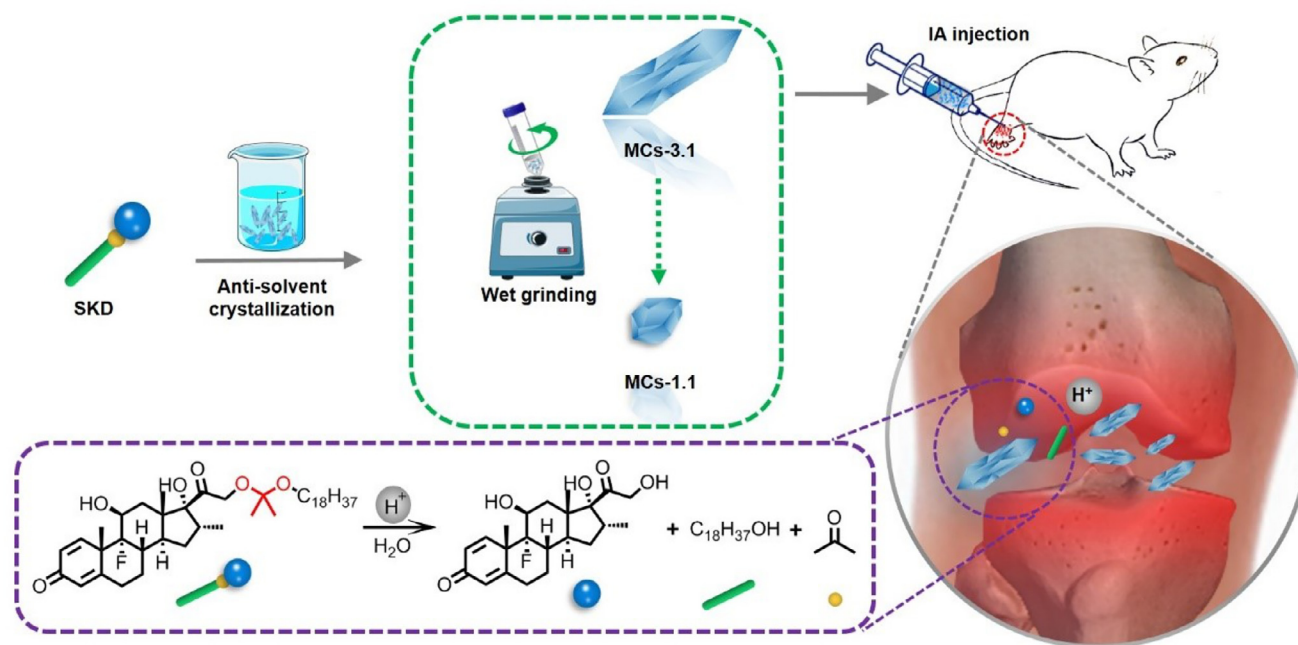
Scheme 1 – Preparation of SKD MCs: the larger MCs were formulated by anti-solvent crystallization method and the smaller ones were further fabricated by wet grinding of larger MCs. In a CIA rat model, MCs exhibited sustained release of native dexamethasone, biocompatible stearyl alcohol and the metabolite acetone in the acidic inflammatory joints post IA injection.

Compared to other administration routes, intra-articular (IA) injection has many advantages, such as maximized drug bioavailability and minimized systemic side effects [9], and IA glucocorticoid injection has been proven for treatment of chronic arthritis since 1950s [10,11]. However, IA glucocorticoid injection is usually short-lived and does not restrict the progression of arthritis effectively [9]. To extend the retention time, prodrug strategy, an important approach to modulate drugs' physiochemical properties, is considered to be promising [12–14]. For instance, by conjugating drugs with hydrophobic promoieties, the hydrophobic prodrugs can reduce the solubility of the native drugs, and thus are useful for the development of formulations for long-term extended release [15–18]. Due to easy manufacture and long-term retention of microcrystals (MCs), hydrophobic prodrugs, including anti-inflammatory [19], antipsychotic [20], antibacterial [21], and hormone prodrugs [15], have been extensively formulated as MCs for treating chronic diseases [22].

In this study, we fabricated two kinds of MCs of an acid-sensitive stearoxyl-ketal-dexamethasone (SKD) prodrug by anti-solvent crystallization and wet grinding methods (Scheme 1). The morphology, size, melting point and crystalline state of MCs were characterized. *In vitro* hydrolysis behavior and cellular uptake of MCs were investigated. In a collagen-induced arthritis (CIA) rat model, we studied the influence of crystal size and injection dose of MCs on long-term therapeutic effects by arthritis scores, pro-inflammatory cytokine levels, histological analysis and micro-CT analysis. Given the pH in inflammatory joints is acidic, acid-sensitive prodrugs could release drug on demand and maintain low level of active drug after remission of arthritis to prevent its relapse.

2. Materials and methods

2.1. Materials

SKD was prepared according to the previous work [23]. Freund's incomplete adjuvant and Bovine Type II Collagen were purchased from Chondrex (Washington DC, USA). ELISA kits of rat TNF-α and IL-1β were ordered from DAKEWE (Shenzhen, China). Raw 264.7 cell line was obtained from National Center for Nanoscience and Technology (Beijing, China). RPMI1640 medium was purchased from Gibco (Carlsbad, USA). Six-well plates were purchased from NEST Biotechnology (Wuxi, China). Other reagents were obtained from commercial vendors.

2.2. Preparation of SKD MCs

SKD MCs with different sizes (designated as MCs-3.1 and MCs-1.1) were fabricated. The larger SKD MCs (MCs-3.1) were first prepared as the following method. Firstly, 3 mg SKD was dissolved in 300 µl ethanol in a 2-ml centrifuge tube. Then, 600 µl 6.7 mM PBS (pH 8.0) was added dropwise to SKD solution. For obtaining MCs-3.1, the centrifuge tube was placed at 4 °C to allow ethanol to slowly evaporate for 48 h until the ethanol volatilizes completely. Subsequently, 100 µl polysorbate 80 solution (0.5%, w/w) was added as stabilizer [24]. The smaller MCs (MCs-1.1) were then obtained by wet

grinding of MCs-3.1 with 500 mg zirconium oxide beads on a vortex for 6 h at 2000 rpm. MCs were separated from the solvent at 5000 × *g* for 10 min by using a Centrifuge 5810 (Eppendorf, DEU), lyophilized for 48 h, and were stored at -20 °C before use. For *in vivo* use, MCs were dispersed with vehicle solution (6.7 mM PBS containing 0.5% polysorbate 80). For fluorescently labeled MCs (MCs-3.1-DID and MCs-1.1-DID), 3 mg SKD and 30 µg DID were dissolved in 300 µl ethanol in the first step, and they were prepared by above procedures.

2.3. Characterization of SKD MCs

Morphology of MCs was observed using scanning electron microscopy (SEM, Phenom Pro, Phenom, NL). Samples were coated with gold by a sputter coater and imaged using SEM at an acceleration voltage of 10 kV. To determine the size of MCs, 12 images of different view fields were selected, and the major axes of 50 crystals per image were randomly measured. MCs were dispersed with 0.5% polysorbate 80 solution to 1 mg/ml, and size distribution and zeta potentials of MCs (MCs-3.1 and MCs-1.1) were investigated by dynamic light scattering (Zetasizer Nano ZS90, Malvern, UK). All measurements were repeated in triplicate. Melting points of SKD amorphous powder, lyophilized MCs-3.1 and MCs-1.1 were determined using micro melting point apparatus (COSSIM RDY-1, CHN). Note that heating temperature ranged from 100 to 130 °C with a heating rate of 3 °C/min. Melting point of the dexamethasone was obtained from literature [25]. Crystalline states of SKD amorphous powder, lyophilized MCs-3.1 and MCs-1.1 were analyzed using X-ray diffractometer (Model Ultima IV, Rigaku, Japan), which was run over a 2*θ* range of 5°–90° by a step size of 0.02°.

2.4. In vitro hydrolysis

The hydrolysis was performed at three pHs in 50 mM acetate buffer (pH 5.0), 50 mM PB buffer (pH 6.0) and 50 mM PB buffer (pH 7.4). All buffers contain 0.5% polysorbate 80. Lyophilized MCs-3.1 and MCs-1.1 were dispersed with vehicle solution (6.7 mM PBS containing 0.5% polysorbate 80) to 4 mg/ml. 20 µl MCs suspension was mixed with 180 µl hydrolysis buffer in a centrifuge tube and incubated at 37 °C and 120 rpm ($n = 4$). At predetermined time points, 200 µl quenching buffer (100 mM Na_2CO_3/$NaHCO_3$ buffer, pH 10.7) was added into the tube to stop hydrolysis, and 1.2 ml ACN was added to solubilize SKD and hydrolyzed compounds. Then, the samples were centrifugated at 12,000 rpm for 10 min (CENCE TGL-16, China). Concentrations of dexamethasone and SKD were determined using HPLC (Agilent 1260, USA). HPLC analysis was performed at 260 nm wavelength using a Phenomenex Luna C_8 column (5 µm, 150 mm × 4.6 mm). The mobile phase was composed by a mixture of ACN (0.1% TEA) and milliQ H_2O according to the gradient: 0–2.5 min 45% ACN, 2.5–5.0 min 45%-95% ACN, 5.0–14.0 min 95% ACN, 14.0–15.0 min 95%-45% ACN. The flow rate of mobile phase was 2.0 ml/min, and the column temperature was maintained at 30 °C. The calibration curves were linear in the range 0.1–100 µg/ml (Dexamethasone: y = 11.06x–0.259, $R^2 = 0.9999$; SKD: y = 6.39x–0.308, $R^2 = 0.9997$).

2.5. In vitro cellular uptake of MCs by Raw 264.7 cells

Raw 264.7 cells were seeded at a density of 5×10^4 cells/well in 6-well plates and were incubated in a humidified incubator at 37 °C and 5% CO_2 for 24 h. For LPS treated group, medium was changed to fresh medium supplemented with LPS at 100 ng/ml to activate Raw 264.7 cells. After an additional 6 h of incubation, the wells were replaced with 2 ml medium containing MCs-3.1-DID or MCs-1.1-DID at a subtoxic concentration (100 µM), followed by 6 h incubation. Cells were washed 5 times with PBS and fixed with 4% paraformaldehyde. Cell nuclei were stained with DAPI, and cell membrane was stained with DIO. Intracellular localization of MCs was observed using laser scanning confocal microscope (TCS SP8, Leica, DEU).

2.6. In vivo therapeutic efficacy

All animal studies were approved by Animal Care and Ethics Committee of the Institute of Radiation Medicine of the Chinese Academy of Medical Sciences. Male Sprague–Dawley rats (180–200 g) were purchased from SPF Biotechnology Co., Ltd (Beijing, China) and maintained under SPF conditions. To establish CIA model, equal volume of Bovine type II collagen (2 mg/ml) and incomplete Freund's adjuvant were emulsified with a homogenizer. On the first day, rats were injected with 200 µl emulsified reagents at the base of the tail. After 7 d, 100 µl of booster injection was injected at the base of the tail. When symptoms of arthritis fully developed on day 20 after initial induction, CIA rats were divided into five groups ($n = 8$), and then a single dose of MCs suspension was IA injected into the bilateral ankle joints. Five groups were CIA (untreated), MCs-3.1–2.5 mg (2.5 mg/kg eq. dexamethasone), MCs-3.1–1.0 mg (1.0 mg/kg eq. dexamethasone), MCs-1.1–2.5 mg (2.5 mg/kg eq. dexamethasone) and MCs-1.1–1.0 mg (1.0 mg/kg eq. dexamethasone). IA injection day was set as Day 0. Hind paw thickness was measured by electric Vernier Caliper and arthritis scores were recorded by previous standard [23]. On day 28 after the IA injection, rats were sacrificed, and plasma and ankle joints were collected for subsequent analysis.

The levels of the pro-inflammatory cytokine TNF-*α* and IL-1*β* in plasma were measured using ELISA kits according to the standard protocols. The optical density was read at 450 nm on a microplate reader (SPARK, Tecan, CH). Dissected joints were fixed in 4% paraformaldehyde and decalcified completely in formalin-EDTA solution (Solarbio, China). Thin sections (5 µm) were cut and stained with hematoxylin-eosin staining and safranin O-fast green. The stained sections were photographed by microscope (Olympus CX41, Japan) with CCD system (AOR, China). The bone protection was evaluated with a Skyscan 1276 micro-CT system (Bruker, DEU). The dissected ankle joints were scanned with the following parameters: voltage, 70 kV; current, 100 µA; exposure time, 910 ms; resolution, 18 µm; and aluminum filter 0.5 mm. The trabecula of calcaneus was selected as region of interest for micro-CT analysis. The reconstructed 3D images were obtained by CT-Vox or CT-Vol software (Skyscan). The morphometric parameters of trabecular bone, including bone volume fraction (BV/TV, %), trabecular thickness (Tb.Th, mm),
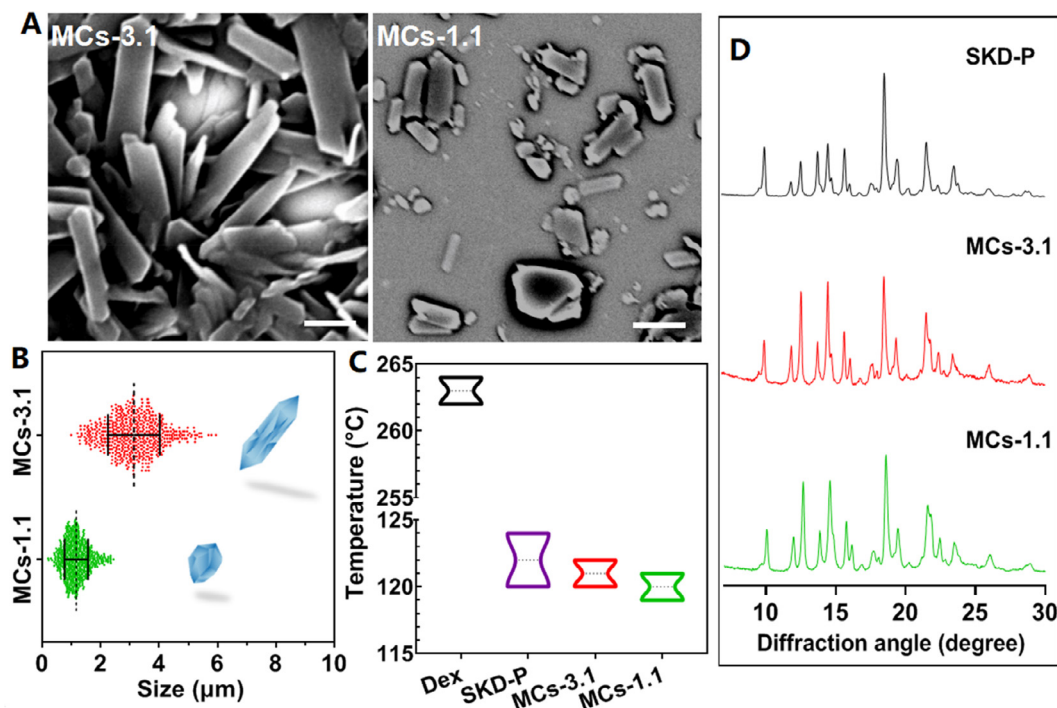
Fig. 1 – Characterizations of SKD MCs. (A) Representative SEM images of MCs-3.1 and MCs-1.1. Scale bar is 1 μm. (B) Statistical size distribution of MCs-3.1 and MCs-1.1. Six hundred of particles were randomly selected from SEM images and their major axes were measured. (C) Melting points of dexamethasone powder (Dex), SKD-P, MCs-3.1 and MCs-1.1, determined by micro melting point apparatus. (D) Representative X-ray diffraction patterns of SKD-P, MCs-3.1 and MCs-1.1.

trabecular number (Tb.N, 1/mm), trabecular separation (Tb.Sp, mm), and structural mode index (SMI), and the mean bone mineral density (BMD) of the calcaneus, were analyzed by software CTAn (Skyscan).

2.7.   Statistical analysis

The data were analyzed using the GraphPad Prism 8 software (GraphPad Software, USA). Differences and correlations between two groups were evaluated for significance using two-tailed unpaired Student's t-test. * $P < 0.05$, ** $P < 0.01$, *** $P < 0.001$ and **** $P < 0.0001$.

3.   Results and discussion

3.1.   Preparation and characterizations of SKD MCs

Using prodrug to reduce drug solubility is a practical strategy for the development of long-acting MCs. In order to reduce the water solubility of dexamethasone, stearyl alcohol, a long hydrophobic alcohol, was conjugated with dexamethasone to form the SKD prodrug. Distinct to previous long-acting ester-based prodrugs, acetone-based ketal is utilized as the linkage for SKD to achieve acid-triggered release. The SKD was synthesized as a white powder, and its MCs were prepared using anti-solvent crystallization method [26]. Here, larger MCs (designated as MCs-3.1) were fabricated at a 1:2 ratio of solvent (ethanol) to anti-solvent (6.7 mM PBS pH 8.0) and

at a SKD concentration of 10 mg/ml in the solvent. After 6 h wet grinding of larger MCs, the smaller MCs (designated as MCs-1.1) were further obtained. Both suspensions of MCs were white emulsions (Fig. S1). According to SEM images (Fig. 1A), microscopic shape of larger MCs was tabular strip, while that of smaller MCs was near-granular shape. To quantify the size of MCs, 600 particles were randomly selected from SEM images and their major axes were measured. The mean size was 3.1 ± 0.8 μm for larger MCs and 1.1 ± 0.4 μm for smaller MCs, respectively (Fig. 1B). Dynamic light scattering analysis (Fig. S2) showed that the sizes of MCs had a normal distribution. Moreover, zeta potentials of MCs-3.1 and MCs-1.1 were -32.5 ± 2.0 mV and -23.0 ± 0.1 mV (Fig. S2), respectively, which are good for stabilizing and re-dispersing MCs in suspensison [27].

As shown in Fig. 1C, the melting point of dexamethasone powder was 262–264 °C, whereas the melting points of SKD formulations were about 120 °C. Specifically, melting points of MCs-3.1 and MCs-1.1 were in the range of 120—122 °C and 119–121 °C, respectively. Moreover, the melting range of amorphous SKD powder (designated as SKD-P) was slightly wider than that of MCs. These results indicate that the crystallinity of SKD MCs was negligibly affected by wet grinding processes. Fig. 1D further showed the X-ray diffraction results of SKD-P, MCs-3.1 and MCs-1.1 in the range of 7°–30° Compared with SKD-P, MCs showed higher crystallinity based on enhanced characteristic peaks intensity at 12.68°, 14.58° and 22.44°, but there was no obvious difference between MCs-3.1 and MCs-1.1. These
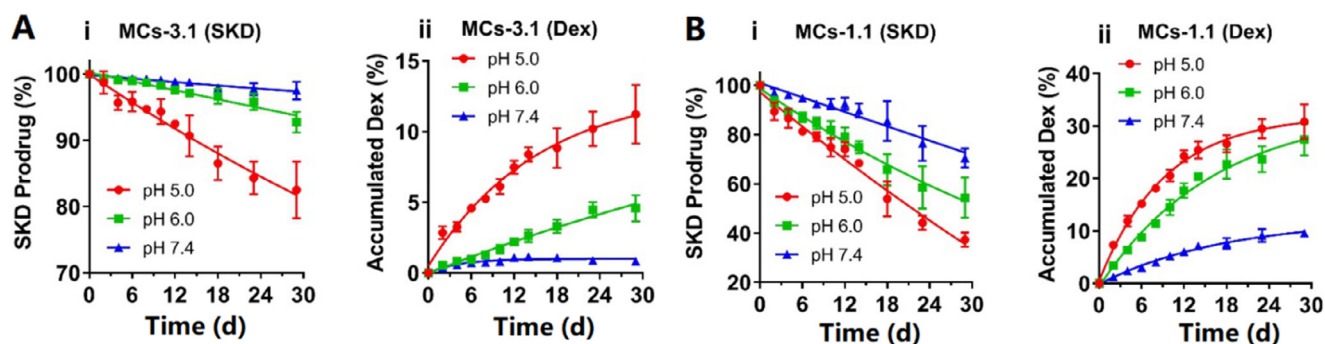
Fig. 2 – *In vitro* hydrolysis: SKD prodrug (%) and accumulated dexamethasone (%) for (A) MCs-3.1 and (B) MCs-1.1 at different pHs. Data are shown as means ± SD ($n = 4$).

results demonstrate that the morphological and physical properties of two kinds of SKD MCs were similar.

3.2. *In vitro hydrolysis*

To investigate *in vitro* hydrolysis of SKD in the MCs, MCs-3.1 and MCs-1.1 were hydrolyzed at three pHs. Fig. 2A-i and Fig. 2B-i showed that SKD MCs underwent a near surface erosion behavior, *i.e.*, hydrolysis of SKD in both MCs followed a near zero-order hydrolysis kinetics. In addition, MCs showed faster hydrolysis at the lower pH and smaller size. Specifically, at pH 5.0, hydrolysis half-life ($T_{1/2}$) was 79 d for MCs-3.1 and 23 d for MCs-1.1, respectively; at pH 6.0, hydrolysis half-life ($T_{1/2}$) was 200 d for MCs-3.1 and 32 d for MCs-1.1, respectively; whereas, at pH 7.4, hydrolysis half-life ($T_{1/2}$) was 581 d for MCs-3.1 and 49 d for MCs-1.1, respectively (Table S1). Fig. 2A-ii and Fig. 2B-ii showed the accumulated dexamethasone (%) after the hydrolysis of SKD. The accumulated amount of dexamethasone was equal to the theoretical amount transformed from the hydrolysis of SKD before Day 10, while the accumulated amount of dexamethasone was less than the theoretical amount after Day 10, because dexamethasone was decomposed over time [28,29]. The above results demonstrated that SKD MCs had slow degradation at physiological pH and had good acid-sensitivity, and thus they are optimal for treatment of chronic arthritis. It is noteworthy that acid-sensitivity of acetone-based ketal-linked prodrugs can be tuned by changing the promoiety, and thus the release duration of MCs may be correspondingly tuned [23].

3.3. *In vitro cellular uptake of MCs by Raw 264.7 cells*

To study the cellular uptake of MCs by Raw 264.7 cells, MCs-3.1 and MCs-1.1 were labeled with fluorescent DID by physical loading [30]. Raw 264.7 cells were incubated with MCs-3.1-DID or MCs-1.1-DID (MCs with DID) and then observed using confocal microscopy. As shown in Fig. 3, MCs displayed red fluorescence which roughly outlined the morphology of the crystals. Compared to LPS untreated cells, LPS-activated Raw 264.7 cells internalized more MCs. There was similar uptake of two kinds of MCs by LPS-activated Raw 264.7 cells, however, MCs-1.1 showed more obvious fluorescence
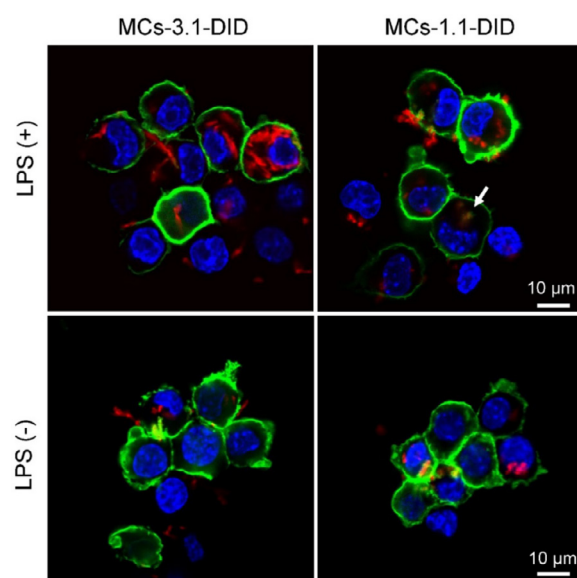
Fig. 3 – Confocal images showed *in vitro* cellular uptake of DID-containing MCs by LPS-stimulated and normal Raw 264.7 macrophages after 6 h of incubation. The green, blue and red color represent cell membrane, nucleus and DID, respectively. The white arrow represents fluorescence dispersion.

dispersion (the white arrow), demonstrating smaller size MCs were more efficiently hydrolyzed in lysosomal acidic environment. We speculate that IA injected MCs will be partially phagocytosed by macrophages at the inflammatory joints to release dexamethasone intracellularly to inhibit inflammation, and those MCs accumulated in macrophages may form a secondary depot for sustained release of dexamethasone [17].

3.4. *In vivo anti-arthritic efficacy*

To examine long-acting therapeutic efficacy of SKD MCs on chronic arthritis, CIA rat model was established [31]. When the inflammation was fully developed with severe swelling, arthritic rats were randomly divided into five groups ($n = 8$)
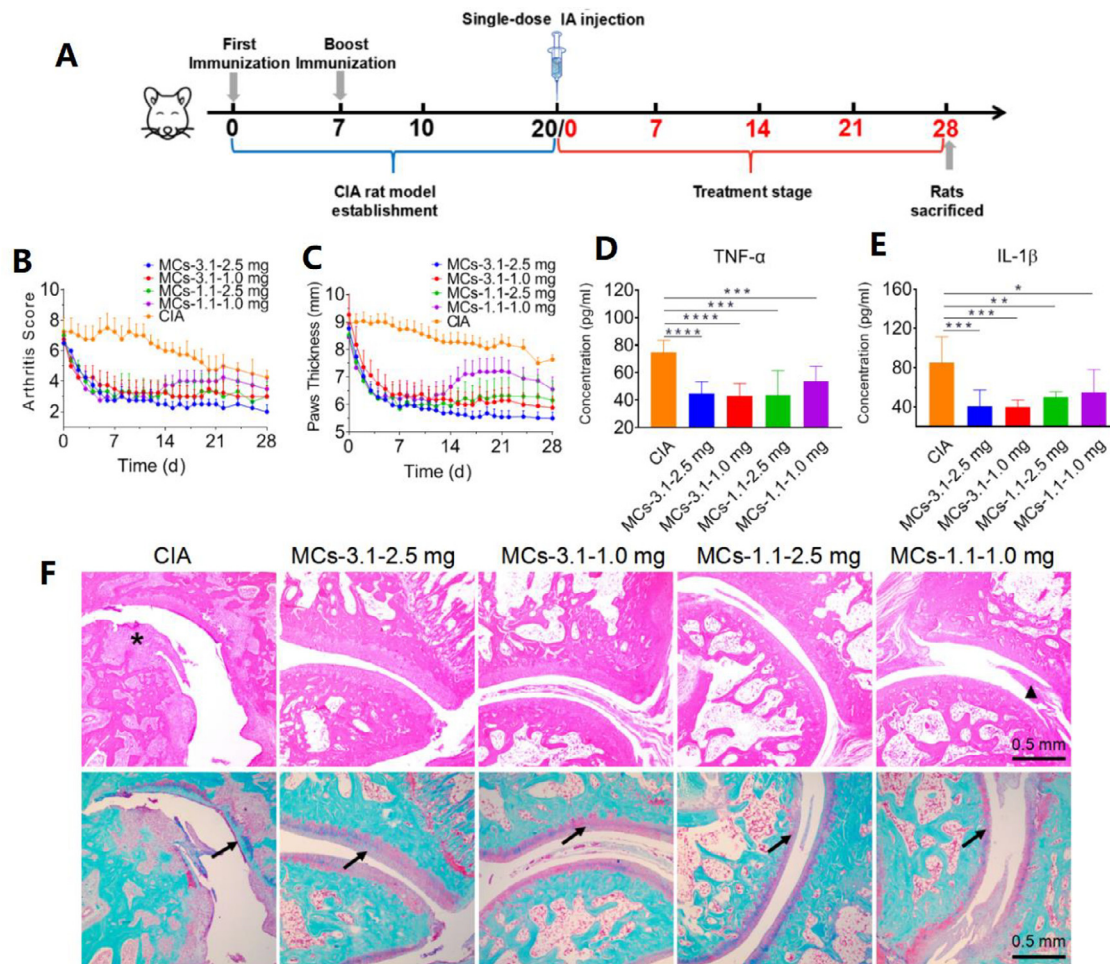
Fig. 4 – Therapeutic effects of MCs in a CIA rat model. (A) Schematic of CIA model establishment and treatment schedules. (B) Arthritis scores and (C) hind paw thickness of rats were recorded from IA injection of MCs to 28 d The plasma levels of (D) TNF-α and (E) IL-1β were measured by ELISA on Day 28 post IA injection. Data are shown as means ± SD ($n = 8$); * $P < 0.05$, ** $P < 0.01$, *** $P < 0.001$, **** $P < 0.0001$. (F) Histological analysis with H&E (upper row) and safranin-O-fast green staining (lower row) of ankle joint tissues from different treatment groups. Arrows show cartilage damage; triangle indicates inflammatory cells infiltration; asterisk shows bone destruction.

and treated with single IA injection of various formulations: MCs-3.1–2.5 mg, MCs-3.1–1.0 mg, MCs-1.1–2.5 mg, and MCs-1.1–1.0 mg (Fig. 4A). Note that 2.5 mg and 1.0 mg represent the injection doses are 2.5 mg/kg eq. dexamethasone and 1.0 mg/kg eq. dexamethasone, respectively. Arthritis scores and paw thickness showed that inflammation of untreated CIA rats remained severe until day 22, after which obvious alleviation occurred (Fig. 4B and 4C). The inflammation in all treatment groups was similarly relieved within 7 days after IA injection. The symptoms began to rebound for MCs-1.1–1.0 mg group from day 14, but still showed significant alleviation compared to untreated CIA group. Other treatment groups showed strong long-acting therapeutic efficacy, and MCs-3.1–2.5 mg group displayed the best anti-arthritic efficacy with paw thickness like normal rats. Therapeutic efficacy of MCs-3.1–1.0 mg group and MCs-1.1–2.5 mg group were relatively lower than that of MCs-3.1–2.5 mg group, while there was no significant difference between these two groups. In the end of treatment, paw thickness of rats treated with MCs-3.1–1.0 mg

and paw thickness of rats treated with MCs-1.1–2.5 mg were quite similar (5.8 ± 1.2 mm *versus* 6.1 ± 1.8 mm).

TNF-α and IL-1β, two pro-inflammatory factors in the progression of RA and OA [32], can be inhibited by dexamethasone treatment. ELISA analysis of two pro-inflammatory cytokines in the plasma on day 28 revealed that the concentrations of TNF-α and IL-1β were reduced by MCs, and lower levels of cytokines were detected in rats treated with MCs-3.1–2.5 mg and MCs-3.1–1.0 mg than that treated with MCs-1.1–1.0 mg and MCs-1.1–2.5 mg (Fig. 4D and 4E). Chronic arthritis manifests as synovitis, progressive bone and cartilage damage. Analysis of ankle joint sections by H&E staining revealed the articular cavity was not integral and the bone and cartilage existed severe erosion in rats of CIA group (Fig. 4F). Pathological sections of joints of rats treated with MCs-3.1–2.5 mg, MCs-3.1–1.0 mg and MCs-1.1–2.5 mg showed relatively integral and clear surfaces with occasional inflammatory cells. By contrast, pathological sections of joints of rats treated with MCs-1.1–1.0 mg showed more
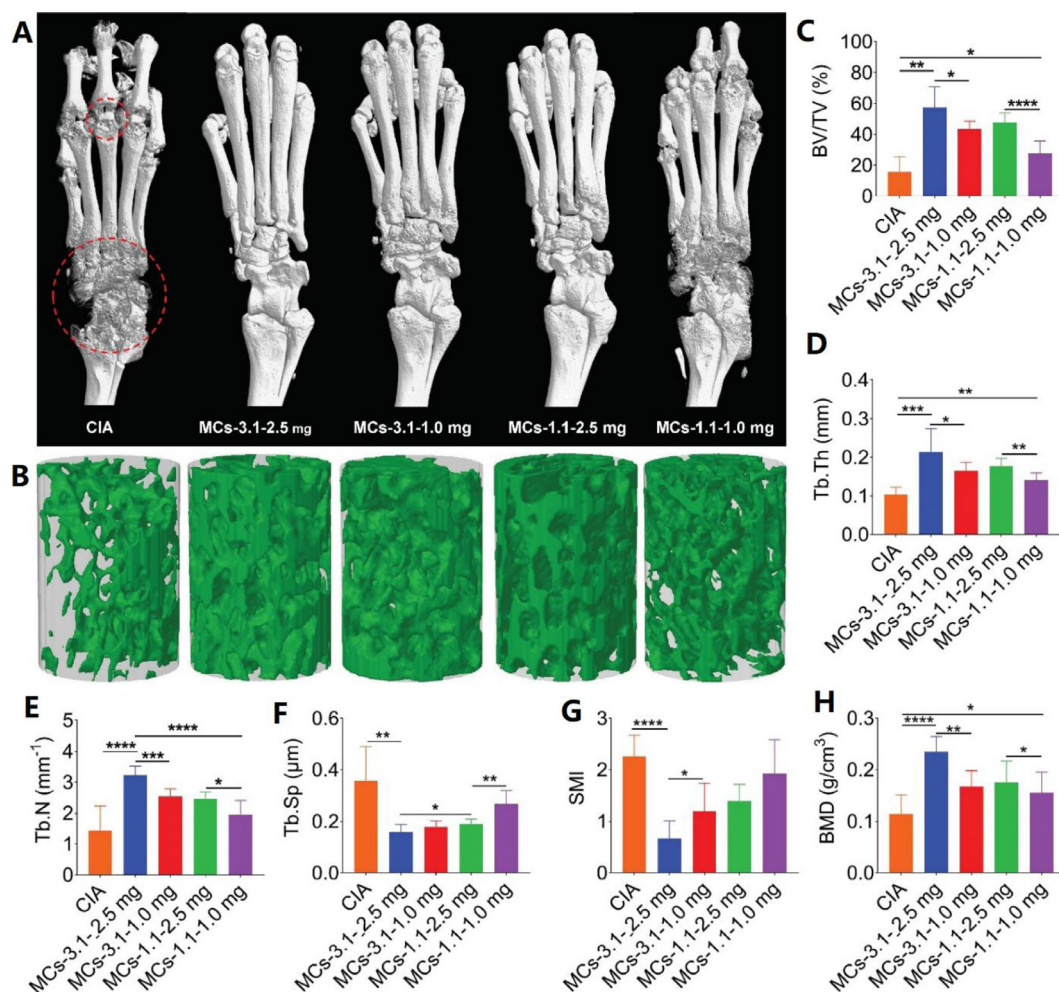
Fig. 5 – Micro-CT analysis. (A) Representative micro-CT images of hind paws. The red circle: bone erosion of ankle and toe joints. (B) 3D trabecular structure of ROI (trabecula of the calcaneus). (C–H) Histomorphometry parameters obtained from analyses of the micro-CT data. BV/TV: bone volume fraction; Tb.Th: trabecular thickness; Tb.N: trabecular number; Tb.Sp: trabecular bone spacing; SMI: structure model index; BMD: bone mineral density. Data are shown as the mean ± SD ($n = 8$); * $P < 0.05$, ** $P < 0.01$, *** $P < 0.001$ and **** $P < 0.0001$.

infiltration of inflammatory cells on the synovial membrane. Pathological sections of joints stained with safranin O-fast green further showed cartilage damage was substantial and nearly undetectable by long-term inflammation from rats of CIA group (Fig. 4F). Articular cartilage of rats treated with MCs-3.1–2.5 mg was well protected, while that of rats treated with MCs-1.1–1.0 mg was significantly eroded.

To evaluate the bone protection of ankle joints, dissected hind paws were evaluated by micro computed tomography (micro-CT). The reconstructed images of cortical bone showed that CIA group existed rough surface and low density of ankle and toe joints. Reduced bone erosion was partially achieved in rats treated with MCs-1.1–1.0 mg, and minor bone erosion was observed in rats treated with MCs-3.1–1.0 mg and MCs-1.1–2.5 mg. Nevertheless, near normal bone surface was observed in MCs-3.1–2.5 mg treated rats (Fig. 5A). Trabecular injury was evaluated by 3D reconstruction of the calcaneus trabecula. Fig. 5B showed that protection of trabeculae in each

treatment group was consistent with that of cortical bone. Quantitative analysis of calcaneus trabeculae convincingly showed protection level from different treatment groups. The calculated parameters reflected morphological information of trabeculae, including BV/TV, Tb.Th, Tb.N, Tb.Sp and SMI (Fig. 5C–5G), which revealed similar therapeutic efficacy results. For example, CIA group had an extremely low BV/TV value (15.7%), whereas four treatment groups increased BV/TV values to 57.4%, 43.5%, 47.5% and 27.3%, respectively. MCs-3.1–2.5 mg group showed the best therapeutic efficacy and there was no significant difference between MCs-3.1–1.0 mg group and MCs-1.1–2.5 mg group. Meanwhile, the highest mean BMD was measured in MCs-3.1–2.5 mg group (Fig. 5H).

One of the side effects of dexamethasone injection is leading to weight loss in rats [33]. After IA injection of SKD MCs, weight loss occurred in all treatment groups, however, the weight of rats gradually began to recover and approached the weight of normal rats after 7 d (Fig. S3). These data

proved the safety of SKD MCs for long-term sustained-release treatment.

Comprehensive analysis of the above results demonstrated that SKD MCs are promising for development of long-acting treatment of chronic arthritis. MCs-3.1–2.5 mg group showed the best long-term anti-inflammatory effect, indicating that high dose of SKD MCs with larger size could release relatively higher concentration of dexamethasone more permanently *in vivo*. However, the smaller size MCs released drug faster and were easier to be eliminated. We envision that SKD MCs can achieve a much longer therapeutic effect in a chronic arthritis model, and relevant studies are ongoing in our laboratory.

4. Conclusion

In summary, we developed MCs formulations of SKD for arthritis treatment. SKD MCs with different sizes (3.1 μm and 1.1 μm) were successfully fabricated by anti-solvent crystallization and wet grinding methods. The melting point and XRD data analysis indicated that the crystallinity of SKD MCs was negligibly affected by wet grinding processes. The MCs showed pH-sensitive hydrolysis *in vitro* and faster hydrolysis at the lower pH and smaller size. They displayed effective treatment of chronic arthritis and safety over one month after single IA injection in CIA rat model, and the size and dosage affected the efficacy. Our studies demonstrate that SKD MCs are promising for development of long-acting treatment of chronic arthritis, and that ketal-based prodrug strategy may be useful for boosting the development of other long-acting formulations, including microcrystals and nanocrystals.

Conflicts of interest

There are no conflicts of interest to declare.

Acknowledgments

Supplementary materials

Supplementary material associated with this article can be found, in the online version, at doi:10.1016/j.ajps.2020.07.002.

REFERENCES

[1] Scott DL, Wolfe F, Huizinga TW. Rheumatoid arthritis. Lancet 2010;376(9746):1094–108.

[2] Collaborators G. Global, regional, and national incidence, prevalence, and years lived with disability for 310 diseases and injuries, 1990–2015: a systematic analysis for the Global Burden of Disease Study 2015. Lancet 2016;388(10053):1545–602.

[3] Carrión M, Frommer KW, Pérez-García S, Müller-Ladner U, Gomariz RP, Neumann E. The adipokine network in rheumatic joint diseases. Int J Mol Sci 2019;20(17):4091.

[4] Jia MD, Deng CF, Luo JW, Zhang P, Sun X. A novel dexamethasone-loaded liposome alleviates rheumatoid arthritis in rats. Int J Pharm 2018;540(1–2):57–64.

[5] Baschant U, Lane NE, Tuckermann J. The multiple facets of glucocorticoid action in rheumatoid arthritis. Nat Rev Rheumatol 2012;8(11):645–55.

[6] Yang M, Feng X, Ding J, Chang F, Chen X. Nanotherapeutics relieve rheumatoid arthritis. J Control Rel 2017;252:108–24.

[7] Mcdonough AK, Curtis JR, Saag KG. The epidemiology of glucocorticoid-associated adverse events. Cur Opin Rheumatol 2008;20(2):131–7.

[8] Saag KG, Koehnke R, Caldwell JR, Brasington R, Burmeister LF, Zimmerman B, et al. Low dose long-term corticosteroid therapy in rheumatoid arthritis: an analysis of serious adverse events. Am J Med 1994;96(2):115–23.

[9] Rai MF, Pham CT. Intra-articular drug delivery systems for joint diseases. Curr Opin Pharmacol 2018;40:67–73.

[10] Hollander JL, Brown EM, Jessar RA, Brown CY. Hydrocortisone and cortisone injected into arthritic joints: comparative effects of and use of hydrocortisone as a local antiarthritic agent. J Am Med Assoc 1951;147(17):1629–35.

[11] Snibbe JC, Gambardella RA. Use of injections for osteoarthritis in joints and sports activity. Clin Sport Med 2005;24(1):83–91.

[12] Zhao Y, Duan S, Zeng X, Liu C, Davies NM, Li B, et al. Prodrug strategy for PSMA-targeted delivery of TGX-221 to prostate cancer cells. Mol Pharm 2012;9(6):1705–16.

[13] Reddy LH, Renoir JM, Marsaud V, Lepetre-Mouelhi S, Desmaële D, Couvreur P. Anticancer efficacy of squalenoyl gemcitabine nanomedicine on 60 human tumor cell panel and on experimental tumor. Mol Pharm 2009;6(5):1526–35.

[14] Kulkarni TA, Bade AN, Sillman B, Shetty BLD, Wojtkiewicz MS, Gautam N, et al. A year-long extended release nanoformulated cabotegravir prodrug. Nat Mater 2020;19:910–20.

[15] Behre H, Abshagen K, Oettel M, Hubler D, Nieschlag E. Intramuscular injection of testosterone undecanoate for the treatment of male hypogonadism: phase I studies. Eur J Endocrinol 1999;140(5):414–19.

[16] Shah A, Mak D, Davies AM, James S, Botchu R. Musculoskeletal corticosteroid administration: current concepts. J Can Assoc Radiol 2019;70(1):29–36.

[17] Darville N, Van Heerden M, Mariën D, De Meulder M, Rossenu S, Vermeulen A, et al. The effect of macrophage and angiogenesis inhibition on the drug release and absorption from an intramuscular sustained-release paliperidone palmitate suspension. J Control Rel 2016;230:95–108.

[18] Park EJ, Amatya S, Kim MS, Park JH, Seol E, Lee H, et al. Long-acting injectable formulations of antipsychotic drugs for the treatment of schizophrenia. Arch Pharm Res 2013;36(6):651–9.

[19] Hu L, Yang C, Kong D, Hu Q, Gao N, Zhai F. Development of a long-acting intramuscularly injectable formulation with nanosuspension of andrographolide. J. Drug Deliv Sci Technol 2016;35:327–32.

[20] Chue P, Chue J. A review of paliperidone palmitate. Expert Opin Drug Deliv 2012;12(12):1383–97.

[21] Tucker I, Jain R, Alawi F, Nanjan K, Bork O. Translational studies on a ready-to-use intramuscular injection of penethamate for bovine mastitis. Drug Deliv Transl Res 2018;8(2):317–28.

[22] Ma Z, Zhang H, Wang Y, Tang X. Development and evaluation of intramuscularly administered nano/microcrystal suspension. Expert Opin Drug Deliv 2019;16(4):347–61.

[23] Xu Y, Mu J, Xu Z, Zhong H, Chen Z, Ni Q, et al. Modular acid-activatable acetone-based ketal-linked nanomedicine by dexamethasone prodrugs for enhanced anti-rheumatoid arthritis with low side effects. Nano Lett 2020;20(4):2558–68.

[[24] Li Y, Sun S, Chang Q, Zhang L, Wang G, Chen W, et al. A strategy for the improvement of the bioavailability and antiosteoporosis activity of BCS IV flavonoid glycosides through the formulation of their lipophilic aglycone into nanocrystals. Mol Pharm 2013;10(7):2534–42.

[25] Milne G.W.A. Drugs: synonyms and properties. 2000:1280.

[26] Maudens P, Seemayer CA, Pfefferlé F, Jordan O, Allémann E. Nanocrystals of a potent p38 MAPK inhibitor embedded in microparticles: therapeutic effects in inflammatory and mechanistic murine models of osteoarthritis. J Control Rel 2018;276:102–12.

[27] Leng D, Chen H, Li G, Guo M, Zhu Z, Xu L, et al. Development and comparison of intramuscularly long-acting paliperidone palmitate nanosuspensions with different particle size. Int J Pharm 2014;472(1–2):380–5.

[28] Matter B, Ghaffari A, Bourne D, Wang Y, Choi S, Kompella UB. Dexamethasone degradation in aqueous medium and implications for correction of in vitro release from sustained release delivery systems. AAPS PharmSciTech 2019;20(8):320.

[29] Hickey T, Kreutzer D, Burgess D, Moussy F. Dexamethasone/PLGA microspheres for continuous delivery of an anti-inflammatory drug for implantable medical devices. Biomaterials 2002;23(7):1649–56.

[30] Chen TK, Li CW, Li Y, Yi X, Lee SMY, Zheng Y. Oral delivery of a nanocrystal formulation of schisantherin a with improved bioavailability and brain delivery for the treatment of Parkinson's disease. Mol Pharm 2016;13(11):3864–75.

[31] Seo J, Park SH, Kim MJ, Ju HJ, Yin XY, Min BH, et al. Injectable click-crosslinked hyaluronic acid depot to prolong therapeutic activity in articular joints affected by rheumatoid arthritis. ACS Appl Mater Interfaces 2019;11(28):24984–98.

[32] Zhang QZ, Dehaini D, Zhang Y, Zhou J, Chen XY, Zhang LF, et al. Neutrophil membrane-coated nanoparticles inhibit synovial inflammation and alleviate joint damage in inflammatory arthritis. Nat Nanotechnol 2018;13(12):1182–90.

[33] Michel C, Cabanac M. Effects of dexamethasone on the body weight set point of rats. Physiol Behav 1999;68(1–2):0–150.